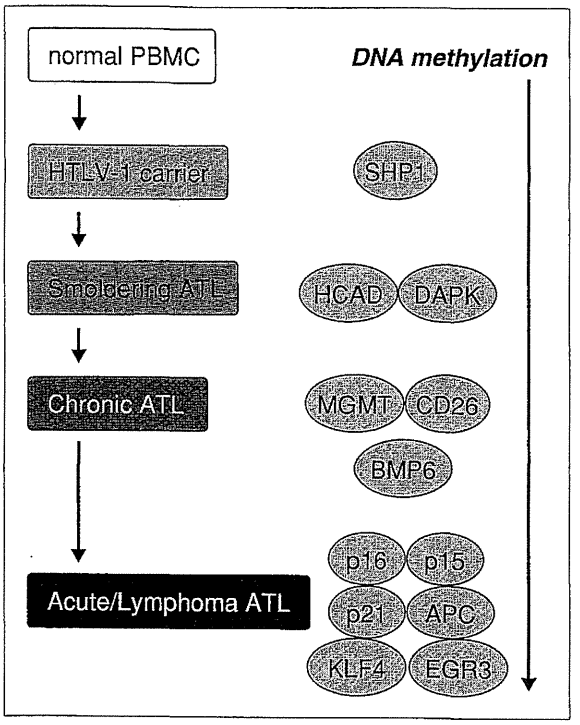

図2　ATLにおけるDNAメチル化の変遷
個々の解析結果を図示した．感染細胞からATL細胞への過程でさまざまな遺伝子のメチル化が獲得される．メチル化された遺伝子は発現が抑制され，細胞周期制御の破綻やアポトーシス抵抗性に寄与する．

おいても機能的な検討が必要であろう．

ATLの進行に伴う遺伝子発現の減少としては*CD26*遺伝子が知られている．この表面マーカーはATL腫瘍細胞で発現が欠失しており，正常Tリンパ球との区別に有用であるが，この*CD26*遺伝子の発現減少にDNAメチル化がかかわっていることが報告されており[12]，病気の進行に伴うDNAのメチル化の獲得が示唆されている．

Methylated CpG-island amplification/representational difference analysis(MCA/RDA)によるDNAのメチル化サイトと脱メチル化サイトのスクリーニングにより，Yasunagaらは53遺伝子の異常なDNAメチル化を明らかにしている[13]．その中には，*KLF4*や*EGR3*といったアポトーシス抵抗性遺伝子が含まれている．また逆にDNAの脱メチル化についても，同研究グループは*MEL1*遺伝子のalternative splicing遺伝子である*MEL1S*が異常な脱メチル化によってATL細胞で発現していることを明らかにしている[14]．またMEL1Sの発現はT細胞株のTGF-βによる増殖抑制を阻害することを示している．

以上より，DNAメチル化のパターンの変化はATL細胞の分子レベルの特徴の一つであり，そのことが細胞レベルの特性に関与していることも明らかである(図2)．しかし前述のとおりDNAメチル化の全体的な解析は行われておらず，またDNAメチル化の制御にかかわる遺伝子異常も報告されていない．近年の網羅的解析技術を駆使して，腫瘍細胞の特徴にかかわるDNAのメチル化パターンを明らかにすることが今後の重要なポイントである．

ATLにおけるヒストン修飾の異常

ヒストンの化学修飾は非常に多くのバリエーションがあり，ATLにおいても複雑な制御機構の逸脱が予想されているが，メチル化DNA解析に比べて臨床検体の調製の難易度が高く，したがって全体的な回答は得られていない．しかし，研究が先行しているヒストン脱アセチル化酵素(HDAC)については，その異常と細胞特性への関与が報告されている．

エピジェネティックな解析で強力なツールとなるのが阻害剤による検討である．Nishiokaらは複数のHDAC阻害剤を用いてHTLV-1感染細胞株を評価し，アポトーシスが誘導されることを明らかにしている[15]．興味深いことにHTLV-1感染細胞で恒常的に活性化しているNF-κB経路がHDAC阻害剤の処理によって抑制されると報告している．しかしHDAC阻害剤は，NF-κB経路のRelAのアセチル化を誘導することによって逆に活性化させるという報告もあり[16]，詳しい分子メカニズムの解析が必要である．

CpGアイランドを持つ遺伝子の多くは，実際にはヒストンのアセチル化とDNAのメチル化が協調して遺伝子発現を抑制することが多い．たとえばTBP-2遺伝子はHTLV-1感染細胞のtransformationの過程で，DNAのメチル化とヒストンの脱アセチル化によって発現が抑制される遺伝子である[17]．TBP-2はHTLV-1感染細胞の増殖を抑制することから[18]，ATL細胞の増殖能に対してエピジェネティックな脱制御が直接的にかかわっていると考えられる．最近新しいHDAC阻害剤であるAR42がATLのマウスモデルに対して有効であることが報告された[19]．毒性の試験や標的遺伝

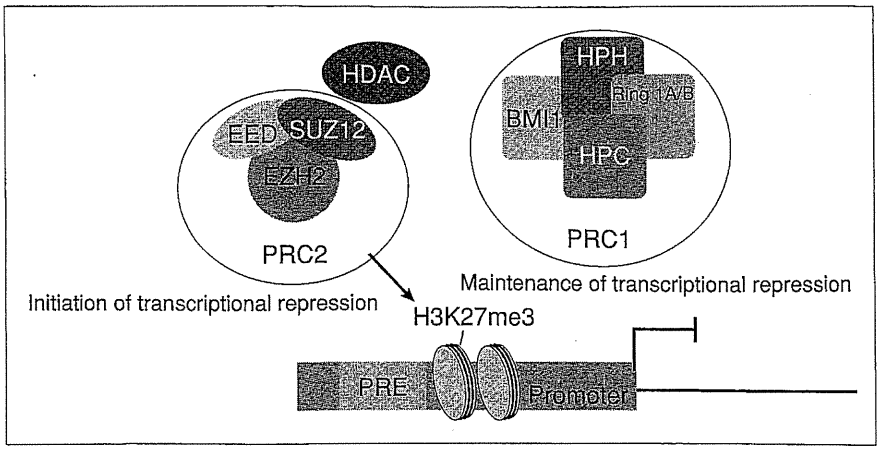

図3　Polycombファミリーによる遺伝子発現制御機構
PRC1とPRC2によりプロモーター上のヒストンH3K27のメチル化が制御され，クロマチンの凝集が起こり，遺伝子発現が抑制される．

子の同定を含む詳細な分子メカニズムの解明が待たれる．

アセチル化に加えて，最近のがん研究において特に研究が進められているのが，ヒストンH3K27のメチル化である．これは，制御する因子群の発現異常や遺伝子変異が多くのがんで同定されていることに起因する．乳がんや前立腺がんなどの固形腫瘍に加え，多くのB細胞リンパ腫において，腫瘍細胞の生存，増殖，脱分化，転移浸潤能と相関することが知られている[20]．H3K27のトリメチル化は主にユークロマチン領域において遺伝子発現の抑制マーカーとして機能する．PolycombファミリーはH3K27のメチル化を制御する因子群であり，これまで長年の研究から，Polycomb repressive complex 1(PRC1)とPRC2という別の複合体がそれぞれ，抑制クロマチン構造の維持と，メチル化導入の役割を担っている(図3)[21]．また，細胞の分化に深くかかわっている分子群として同定されており，造血幹細胞の制御にも重要である．

ATLにおけるPolycombファミリーの異常は，網羅的遺伝子発現解析によって明らかにされた[4)22)]．なかでもH3K27のメチル化酵素であるEZH2の過剰発現が顕著であり，細胞全体のメチル化H3K27me3レベルの亢進も検出されている．EZH2の阻害剤であるDZNep処理によりATL細胞株のアポトーシスが誘導されることから，Polycombの発現異常がATL細胞の生存にかかわることが示されている[22]．またHDAC阻害剤との併用がより効果的であったことは，複雑なエピゲノムの脱制御がATL細胞の背景にあることを示唆している．

ATL細胞のエピゲノム異常と細胞生存シグナルへの関与

われわれはATL細胞の分子病態の全体像をつかむために，HTLV-1感染者コホート共同研究班(JSPFAD)の全面的協力を得て，ATL 52例と健常人CD4陽性T細胞21例の網羅的遺伝子発現解析を行った．加えて，miRNA発現およびゲノムDNAコピー数の大規模な統合解析を行うことによって，ATL細胞の分子レベルの全体像をデータとして取得することに成功した[4]．

ATLにおいて，Polycombファミリーに属する遺伝子群で顕著に異常を示したのが，EZH2およびSUZ12であった(表1)．いずれもPRC2の構成因子であり，その過剰発現はPRC2の酵素活性を上昇させ，異常なメチル化パターンが誘導されることが他の腫瘍で報告されている．われわれはさらに，これらの生物学的意義を明らかにするために多角的に検証した結果，ATL細胞におけるPolycombファミリーの発現異常ががん抑制性miRNAのサイレンシングにかかわっていることを明らかにした．

miRNAは遺伝子発現全体に対して“Fine tuner”として機能する分子群であり，がんやウイルス感染症を考える上でも欠かすことのできない因子として位置づけられている．miRNAによる遺

表1　ATL細胞におけるPolycombファミリーの発現変化

Gene (PcG subunits)	PcG subunits in *Drosophila melanogaser*	PcG complex in humans	Fold change (ATL/Normal)	*P* value
CBX2	Polycomb	PRC1	—	—
CBX4			1.648	1.09×10^{-6}
CBX6			0.828	0.00258
CBX7			—	—
CBX8			2.363	4.80×10^{-9}
PHC1	Polyhomeotic		2.031	1.19×10^{-5}
PHC2			1.389	9.45×10^{-5}
BMI1	Posterior Sex combs		1.584	5.01×10^{-6}
MEL18			—	—
NSPC1			—	—
RING1	Sex combs extra		—	—
RING1B			0.646	1.36×10^{-6}
EZH1	Enhancer of Zeste	PRC2	—	—
EZH2			2.827	1.90×10^{-15}
SUZ12	Suppressor of Zeste 12		2.049	4.94×10^{-16}
EED	Extra Sex combs		1.465 (EED2)	3.29×10^{-7}
RbAp48	Nucleosome remodeling factor 55		1.605	1.25×10^{-9}
RbAp46			1.245	0.00248
PHF1	Polycomb-like	Binds PRC2	—	—
MTF2			—	—
PHF19			—	—
YY1	Pleiohomeotic	PHORC	—	—
RYBP			1.681	2.70×10^{-6}

ATL検体を用いた網羅的遺伝子発現解析の結果．正常CD4陽性T細胞と比較した発現量の変化を示した．
（文献[4]から引用，一部改変）

伝子発現制御機構の詳細は他の文献を参考されたい[23]．特筆すべきは，miRNAの存在が示されて以降，遺伝子発現制御研究は飛躍的に進展したことである．

ATL, HTLV-1関連分野においてもmiRNAの異常が示唆されていたが，その実態は不明であった．われわれはATL細胞の分子病態の全体像をつかむために，ATL 40例，健常人CD4陽性T細胞22例についてmiRNAの網羅的解析を行った結果，ATLでは61種のmiRNAが異常発現を示し，そのうち59種のmiRNAが正常T細胞に比べて低値を示すことがわかった．これは，腫瘍細胞はmiRNAの発現が全体的に低下傾向にあるという他のがん研究の結果と一致している．これらのmiRNAはATL細胞の新たな分子マーカーであり，またひとつひとつが腫瘍細胞の特徴に寄与していると考えられる．

61種の発現異常miRNAのうち，miR-31が例外なくすべてのATL患者で著しく減少していた（図4）．miR-31の発現減少は，乳がんにおける転移，浸潤過程において重要であることが報告されている[24]．われわれは，miR-31の著しい減少がATL細胞の特徴を反映していると考え，ATL細胞のmRNA発現プロファイルの結果と統合し，さらに*in vitro*の複数の実験を経て，ATL細胞におけるNF-κB活性化の原因遺伝子であるNIKがmiR-31の新規標的遺伝子であることを見出した．実験の結果，正常T細胞ではmiR-31の発現が比較的高くNIKの発現を抑制しているが，miR-31の異常な発現低下がNIKの発現誘導とそれに伴うNF-κB経路の恒常的活性化を誘発することがわかった．さらにATL細胞株および新鮮ATL細胞に対してmiR-31を再導入すると細胞死が誘導された．このことは，miR-31の細胞内レベルが腫瘍細胞の表現型に直接影響していることを意味し，新しい分子標的としての有用性が示された．

ATL臨床検体を詳細に解析した結果，ゲノムの欠損と上述したPolycombファミリー依存的なエピジェネティックな異常によって，miR-31の発現欠失がすべてのATL患者で起こっていることが

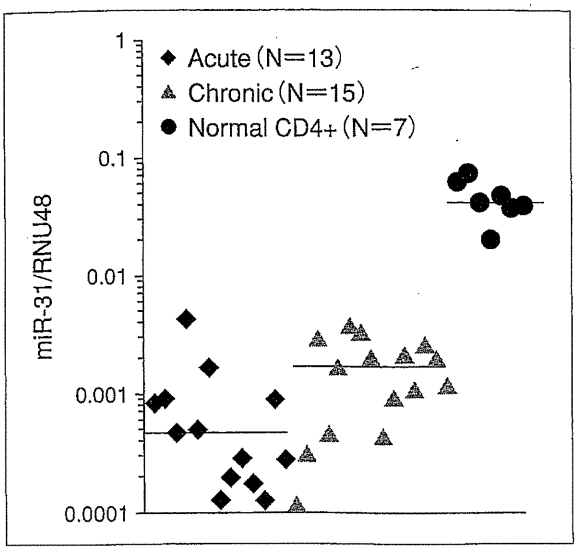

図4　ATLにおけるmiR-31の発現低下
Real-time PCRによるmiR-31の定量結果．miR-31の発現は例外なくATLで発現が低下している．

わかった．さらに，PolycombファミリーがmiR-31を抑制することによってNIK−NF-κB経路を活性化する分子機構は，ATLだけでなく乳がん細胞やB細胞における免疫応答反応においても保存されていた．Polycombファミリー，NF-κB経路，miR-31はそれぞれが単独で，おのおのの多彩な機能によって細胞の恒常性や分化などのさまざまなプロセスにかかわると同時に，さらにクロストークを形成することによって，より複雑な遺伝子発現制御ネットワークを形成していると考えられる(図5)[4]．われわれの実験結果は，長らく不明であったATL細胞におけるNF-κB経路の恒常的活性化の詳細な分子機構を明らかにした[3]．ATL細胞はこの分子ネットワークの異常に依存しており，Polycombの制御，もしくはmiR-31の補充による新たな治療法の開発につながると期待される．

Polycombファミリーについては，造血器腫瘍において非常に盛んに研究が進められている分子群である．ほとんどすべてのB細胞リンパ腫において過剰に発現しており[25]，またさらに一部の腫瘍においてはgain-of-function mutationも報告されていることもあり，治療標的としても注目を浴びている[26]．しかし一方で未分化な白血病細胞では逆にがん抑制性遺伝子として機能していることも明らかとなり[27]，分化段階とPolycombによるエピジェネティック制御は今後さらに研究が加速すると考えられる．

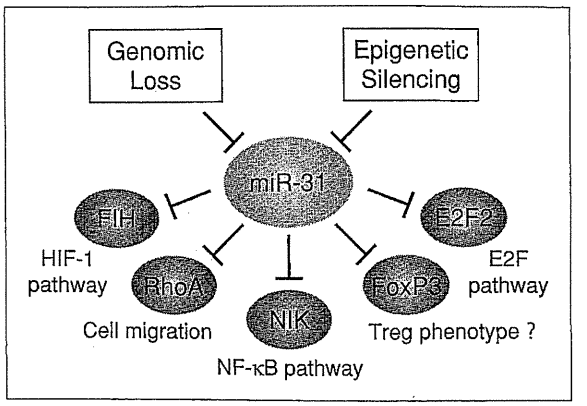

図5　ATL細胞における新たな分子メカニズム
遺伝子の欠損とPolycomb依存的なエピジェネティックな異常によってmiR-31の発現が低下すると，NIKなどの標的遺伝子の発現抑制が解除され，細胞内のシグナル伝達経路が攪乱される．この分子メカニズムは他のがん細胞でも保存されている．

HTLV-1感染による宿主エピゲノムへの影響

ATL細胞のエピゲノムの異常の実態が少しずつ明らかになっている一方で，どのような過程を経て異常パターンを獲得するのかについてはほとんど明らかではない．しかし実験的証拠として，ウイルス遺伝子産物であるTaxが宿主T細胞のエピジェネティック調節因子に結合し，影響を与えることが複数示されている．

TaxはHDAC1と相互作用し，プロウイルスの制御を担うと同時に，宿主に対しても影響を与えることが示唆されている[28]．またわれわれはTaxとヒストンメチル化酵素であるSUV39H1やSMYD3との物理的な相互作用を発見した[29][30]．終末像であるATL細胞のエピゲノムの異常の維持と特性を明らかにするとともに，HTLV-1感染細胞からATL細胞への進展を考える上で，包括的なエピゲノム解析と詳細な分子機構の解明が急務であろう．

今後の展望

ゲノム，エピゲノムの異常を背景として，細胞周期の脱制御，miRNAの発現低下，シグナル伝達経路の恒常的活性化がこれまでに明らかになっているATL細胞の分子レベルの特徴である(図6)．miRNAの全体的な発現低下に対して，エピゲノ

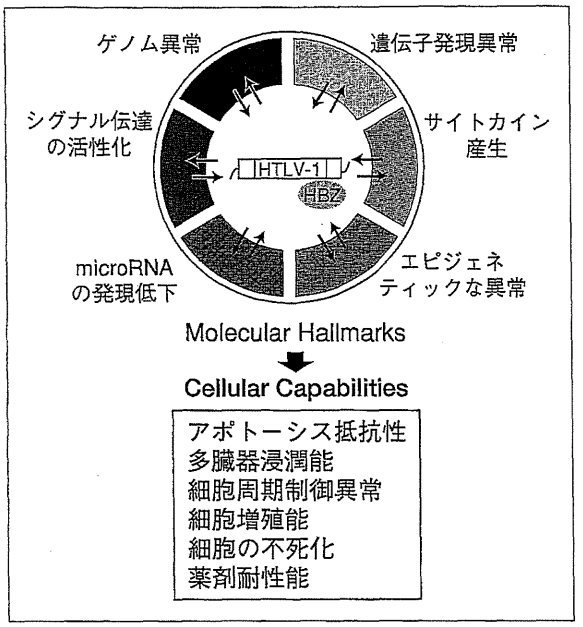

図6　ATL細胞における分子レベルの特徴
大規模解析結果からみるATLの分子レベルの特徴を概略図として示した．HTLV-1感染細胞がさまざまな分子異常を獲得し，悪性度の高い腫瘍細胞の特徴に寄与する．　（文献[3]より引用，一部改変）

ムの脱制御がどのようにかかわっているのかは，非常に興味深い課題である．今後は，これまでの感染細胞株や終末像である新鮮ATL細胞の詳細なデータをまとめ，感染細胞の恒常性の破綻，感染クローンの変遷，発症や薬剤耐性の分子メカニズム，などに対するエピゲノムの異常のかかわりについて取り組む必要があるであろう．

文　献

1) Yamaguchi K, Watanabe T. Human T lymphotropic virus type-I and adult T-cell leukemia in Japan. Int J Hematol 2002 ; 76 Suppl 2 : 240.
2) Matsuoka M, Jeang KT. Human T-cell leukaemia virus type 1 (HTLV-1) infectivity and cellular transformation. Nat Rev Cancer 2007 ; 7 : 270.
3) Yamagishi M, Watanabe T. Molecular hallmarks of adult T cell leukemia. Front Microbiol 2012 ; 3 : 334.
4) Yamagishi M, Nakano K, Miyake A, et al. Polycomb-mediated loss of miR-31 activates NIK-dependent NF-κB pathway in adult T cell leukemia and other cancers. Cancer Cell 2012 ; 21 : 121.
5) Yamagishi M, Watanabe T. New paradigm of T cell signaling : learning from malignancies. J Clin Cell Immunol 2012 ; S12 : 007.
6) Nosaka K, Maeda M, Tamiya S, et al. Increasing methylation of the CDKN2A gene is associated with the progression of adult T-cell leukemia. Cancer Res 2000 ; 60 : 1043.
7) Hofmann WK, Tsukasaki K, Takeuchi N, et al. Methylation analysis of cell cycle control genes in adult T-cell leukemia/lymphoma. Leuk Lymphoma 2001 ; 42 : 1107.
8) Sato H, Oka T, Shinnou Y, et al. Multi-step aberrant CpG island hyper-methylation is associated with the progression of adult T-cell leukemia/lymphoma. Am J Pathol 2010 ; 176 : 402.
9) Watanabe M, Nakahata S, Hamasaki M, et al. Downregulation of CDKN1A in adult T-cell leukemia/lymphoma despite overexpression of CDKN1A in human T-lymphotropic virus 1-infected cell lines. J Virol 2010 ; 84 : 6966.
10) Taniguchi A, Nemoto Y, Yokoyama A, et al. Promoter methylation of the bone morphogenetic protein-6 gene in association with adult T-cell leukemia. Int J Cancer 2008 ; 123 : 1824.
11) Yang Y, Takeuchi S, Tsukasaki K, et al. Methylation analysis of the adenomatous polyposis coli (APC) gene in adult T-cell leukemia/lymphoma. Leuk Res 2005 ; 29 : 47.
12) Tsuji T, Sugahara K, Tsuruda K, et al. Clinical and oncologic implications in epigenetic down-regulation of CD26/dipeptidyl peptidase IV in adult T-cell leukemia cells. Int J Hematol 2004 ; 80 : 254.
13) Yasunaga J, Taniguchi Y, Nosaka K, et al. Identification of aberrantly methylated genes in association with adult T-cell leukemia. Cancer Res 2004 ; 64 : 6002.
14) Yoshida M, Nosaka K, Yasunaga J, et al. Aberrant expression of the MEL1S gene identified in association with hypomethylation in adult T-cell leukemia cells. Blood 2004 ; 103 : 2753.
15) Nishioka C, Ikezoe T, Yang J, et al. Histone deacetylase inhibitors induce growth arrest and apoptosis of HTLV-1-infected T-cells via blockade of signaling by nuclear factor kappaB. Leuk Res 2008 ; 32 : 287.

16) Chiechio S, Zammataro M, Morales ME, et al. Epigenetic modulation of mGlu2 receptors by histone deacetylase inhibitors in the treatment of inflammatory pain. Mol Pharmacol 2009 ; 75 : 1014.
17) Ahsan MK, Masutani H, Yamaguchi Y, et al. Loss of interleukin-2-dependency in HTLV-I-infected T cells on gene silencing of thioredoxin-binding protein-2. Oncogene 2006 ; 25 : 2181.
18) Nishinaka Y, Nishiyama A, Masutani H, et al. Loss of thioredoxin-binding protein-2/vitamin D3 up-regulated protein 1 in human T-cell leukemia virus type I-dependent T-cell transformation : implications for adult T-cell leukemia leukemogenesis. Cancer Res 2004 ; 64 : 1287.
19) Zimmerman B, Sargeant A, Landes K, et al. Efficacy of novel histone deacetylase inhibitor, AR42, in a mouse model of, human T-lymphotropic virus type 1 adult T cell lymphoma. Leuk Res 2011 ; 35 : 1491.
20) Sparmann A, van Lohuizen M. Polycomb silencers control cell fate, development and cancer. Nat Rev Cancer 2006 ; 6 : 846.
21) Schuettengruber B, Chourrout D, Vervoort M, et al. Genome regulation by polycomb and trithorax proteins. Cell 2007 ; 128 : 735.
22) Sasaki D, Imaizumi Y, Hasegawa H, et al. Overexpression of Enhancer of zeste homolog 2 with trimethylation of lysine 27 on histone H3 in adult T-cell leukemia/lymphoma as a target for epigenetic therapy. Haematologica 2011 ; 96 : 712.
23) He L, Hannon GJ. MicroRNAs : small RNAs with a big role in gene regulation. Nat Rev Genet 2004 ; 5 : 522.
24) Valastyan S, Reinhardt F, Benaich N, et al. A pleiotropically acting microRNA, miR-31, inhibits breast cancer metastasis. Cell 2009 ; 137 : 1032.
25) Martin-Perez D, Piris MA, Sanchez-Beato M. Polycomb proteins in hematologic malignancies. Blood 2010 ; 116 : 5465.
26) McCabe MT, Ott HM, Ganji G, et al. EZH2 inhibition as a therapeutic strategy for lymphoma with EZH2-activating mutations. Nature 2012 ; 492 : 108.
27) Hock H. A complex Polycomb issue : the two faces of EZH2 in cancer. Genes Dev 2012 ; 26 : 751.
28) Ego T, Ariumi Y, Shimotohno K. The interaction of HTLV-1 Tax with HDAC1 negatively regulates the viral gene expression. Oncogene 2002 ; 21 : 7241.
29) Kamoi K, Yamamoto K, Misawa A, et al. SUV39H1 interacts with HTLV-1 Tax and abrogates Tax transactivation of HTLV-1 LTR. Retrovirology 2006 ; 3 : 5.
30) Yamamoto K, Ishida T, Nakano K, et al. SMYD3 interacts with HTLV-1 Tax and regulates subcellular localization of Tax. Cancer Sci 2011 ; 102 : 260.

* * *

Cancer Science
The official journal of the Japanese Cancer Association JCA

Adult T-cell leukemia cells are characterized by abnormalities of *Helios* expression that promote T cell growth

Satomi Asanuma,[1] Makoto Yamagishi,[1] Katsuaki Kawanami,[1] Kazumi Nakano,[1] Aiko Sato-Otsubo,[2] Satsuki Muto,[2] Masashi Sanada,[2] Tadanori Yamochi,[1] Seiichiro Kobayashi,[3] Atae Utsunomiya,[4] Masako Iwanaga,[5] Kazunari Yamaguchi,[6] Kaoru Uchimaru,[3] Seishi Ogawa[2] and Toshiki Watanabe[1,7]

[1]Graduate School of Frontier Sciences, The University of Tokyo; [2]Cancer Genomics Project, Graduate School of Medicine, The University of Tokyo; [3]Institute of Medical Science, The University of Tokyo, Tokyo; [4]Department of Hematology, Imamura Bun-in Hospital, Kagoshima; [5]Graduate School of Public Health, Teikyo University; [6]Department of Safety Research on Blood and Biological Products, National Institute of Infectious Diseases, Tokyo, Japan

(Received December 27, 2012/Revised April 11, 2013/Accepted April 15, 2013/Accepted manuscript online April 18, 2013/Article first published online May 19, 2013)

Molecular abnormalities involved in the multistep leukemogenesis of adult T-cell leukemia (ATL) remain to be clarified. Based on our integrated database, we focused on the expression patterns and levels of Ikaros family genes, *Ikaros*, *Helios*, and *Aiolos*, in ATL patients and HTLV-1 carriers. The results revealed profound deregulation of Helios expression, a pivotal regulator in the control of T-cell differentiation and activation. The majority of ATL samples (32/37 cases) showed abnormal splicing of Helios expression, and four cases did not express Helios. In addition, novel genomic loss in *Helios* locus was observed in 17/168 cases. We identified four ATL-specific short Helios isoforms and revealed their dominant-negative function. Ectopic expression of ATL-type Helios isoform as well as knockdown of normal Helios or Ikaros promoted T-cell growth. Global mRNA profiling and pathway analysis showed activation of several signaling pathways important for lymphocyte proliferation and survival. These data provide new insights into the molecular involvement of Helios function in the leukemogenesis and phenotype of ATL cells, indicating that Helios deregulation is one of the novel molecular hallmarks of ATL. (*Cancer Sci* 2013; 104: 1097–1106)

Adult T-cell leukemia (ATL) is a highly aggressive malignancy of mature CD4+ T cells and is caused by HTLV-1. After HTLV-1 infection, ATL is thought to develop following a multitude of events, including both genetic and epigenetic changes in the cells. Although many aspects of HTLV-1 biology have been elucidated, the detailed molecular mechanism of ATL leukemogenesis remains largely unknown.[1,2] Therefore, to precisely define the comprehensive abnormalities associated with ATL leukemogenesis, we previously carried out global mRNA and miRNA profiling of ATL cells derived from a large number of patients.[3,4] In this study, we focused on Ikaros family genes, especially Helios, on the basis of our integrated profiling of expression and gene copy number in ATL cells, which revealed the deregulated expression of this family of genes and genomic loss of *Helios* locus.

Ikaros family genes are specifically expressed in the hematopoietic system and play a vital role in regulation of lymphoid development and differentiation.[5–11] In addition, they are known to function as tumor suppressors during leukemogenesis according to several genetic studies carried out in mouse models.[12–15] Recently, many studies reported the deregulated splicing of Ikaros and the deletion of *Ikaros* locus in several human leukemias.[16–23] These abnormalities are associated with poor prognoses.[24–27] Helios is mainly expressed in the T-cell lineage.[10,11] Genomic changes and abnormal expression of Helios are also observed in some patients with T-cell malignancies.[18,28–31] However, in contrast to Ikaros, the substantial impact of aberrant Helios expression remains to be elucidated because of the absence of functional information, including the target genes of Helios.

In this study, we carried out a detailed expression analysis of Ikaros family genes in a large panel of clinical samples from ATL patients and HTLV-1 carriers and consequently identified a novel molecular characteristic, that is, abnormal splicing of Helios and loss of expression, which seems to be a significant key factor in leukemogenesis affecting the regulation of T-cell proliferation.

Materials and Methods

Cell lines and clinical samples. HeLa and 293T cells were cultivated in DMEM supplemented with 10% FCS. Human leukemic T cells, Jurkat, Molt-4, and CEM, ATL-derived, MT-1 and TL-Om1, and HTLV-1-infected MT-2 and Hut-102 cell lines were all maintained in RPMI-1640 with 10% FCS. The PBMCs from ATL patients of four clinical subtypes[32] and healthy volunteers were a part of those collected with informed consent as a collaborative project of the Joint Study on Prognostic Factors of ATL Development. The project was approved by the Institute of Medical Sciences, University of Tokyo Human Genome Research Ethics Committee (Tokyo, Japan). Clinical information of ATL individuals is provided in Table S1.

RNA isolation and RT-PCR analysis. The preparation of total RNA and synthesis of the first strand of cDNA were described previously.[3] The mRNAs of Ikaros family genes were examined by PCR with Platinum Taq DNA Polymerase High Fidelity (Invitrogen, Carlsbad, CA, USA). The PCR products were sequenced by automated DNA sequencer. Nested PCR amplification was carried out with diluted full-length PCR products by Accuprime Taq DNA polymerase High Fidelity (Invitrogen). Quantitative PCR was carried out as previously described.[3] The specific primer sets for each PCR are described in Table S2.

Immunoblot analysis. Cells were collected, washed with PBS, and lysed with RIPA buffer. For immunoprecipitation, cells were lysed with TNE buffer and incubated with specific antibody. Proteins samples were then analyzed by immunoblots with specific antibodies: anti-tubulin, anti-Ikaros, and anti-Helios antibodies were from Santa Cruz Biotechnology (Santa Cruz, CA, USA). Mouse anti-FLAG antibody (M2) was from Sigma-Aldrich (St. Louis, MO, USA). Rabbit polyclonal anti-HA

[7]To whom correspondence should be addressed.
E-mail: tnabe@ims.u-tokyo.ac.jp

doi: 10.1111/cas.12181

antibody was from MBL (Nagoya, Japan). Anti-mouse, rabbit, and goat secondary antibodies were from Promega (Fitchburg, WI, USA).

Immunostaining. HeLa cells were cultured on coverslip slides and transfected with the indicated expression vectors by Lipofectamine LTX (Invitrogen). At 24 h post transfection, cells were washed three times with PBS, fixed in 4% paraformaldehyde, and permeabilized with 0.1% Triton X-100. Then, cells were stained with primary antibodies (diluted 1:500 to 1:2000). Alexa-488 or 546-conjugated secondary antibodies (Molecular Probes, Life Technologies, Carlsbad, CA, USA) were used for detection of specific targets, and DAPI was used for nuclear staining. Images were acquired by using a Nikon A1 confocal microscope (Nikon, Tokyo, Japan).

Electrophoretic mobility-shift assay. Experimental conditions and detail methods were previously reported.[3] For evaluation of DNA binding activity, 3–5 μg nuclear extracts from each transfectant were used per each lane of electrophoresis. The oligonucleotide sequences used as a probe are provided in Table S2.

Luciferase assay. The pGL4.10-firefly vector (Promega) containing *Hes1* promoter was used as a reporter vector and RSV-renilla vector was used as a control vector. HeLa cells were transiently transfected with these reporters and each Ikaros or/and Helios expression vector by Lipofectamine 2000 reagent (Invitrogen). The luciferase activities were quantified by the Dual-Luciferase Reporter Assay System (Promega) at 24 h post-transfection.

Retroviral construction and transduction. The FLAG-Hel-5 cDNA sequence was subcloned into retrovirus vector pRx-puro. Stable cell populations expressing Hel-5 were selected by puromycin. The shRNA-expressing retroviral vectors and virus production procedures have been established.[3] The shRNA sequences are listed in Table S2. Stable cell populations were obtained by puromycin or G418 selection.

Proliferation assays. Cells (0.5 or 1.0×10^4) were plated in 96-well plates with media supplemented with 10% or 0.2% FCS. The cell numbers were evaluated for 4 days by Cell Counting Kit-8 (Dojindo, Kumamoto, Japan). The averages of at least three independent experiments are shown.

Gene expression microarray analyses. Gene expression microarray used the 4×44K Whole Human Genome Oligo Microarray (Agilent Technologies, Santa Clara, CA, USA); detailed methods were previously reported.[3] Coordinates have been deposited in the Gene Expression Omnibus database with accession numbers GSE33615 (gene expression microarray), GSE33602 (copy number analyses), and GSE41796 (Jurkat models).

Results

Abnormal expression of short Helios transcripts in primary ATL cells. To characterize the gene expression signature in primary ATL cells, we previously carried out mRNA microarray analyses on a large number of samples. The comprehensive survey unveiled deregulated expression of Ikaros family genes; transcription levels of Ikaros and Aiolos were downregulated in ATL samples, whereas Helios was upregulated (Fig. S1). Thus, we examined the detailed expression patterns and levels of Ikaros family members in PBMCs derived from a panel of ATL patients and HTLV-1 carriers (Fig. 1a). Compared with control PBMCs from normal volunteers (Fig. 1b), the expression levels of Ikaros and Aiolos seemed to be downregulated in ATL samples, consistent with our microarray results. However, there were obvious abnormalities in the expression patterns of Helios. The main isoform of Helios was changed from full-length Hel-1 to Hel-2, which lacks exon 3 that contains the first N-terminal zinc finger in the DNA-binding domain. In addition, four ATL-specific Helios short transcripts were identified (Fig. 1c). Among them, Hel-5 and Hel-6 have been reported to be expressed in ATL.[29] We also identified two novel variants, Hel-v1 that lacks exons 3 and 4 and Hel-v2 that lacks exons 2, 3, and 6. These abnormal Helios variants were also expressed in the samples of high-risk HTLV-1 carriers, who subsequently developed ATL in the next few years. Furthermore, nested PCR revealed that Hel-5 or Hel-6 were expressed in a majority of ATL samples (17/22 acute cases, 10/10 chronic cases, and 5/5 smoldering cases; total, 32/37 cases) (Fig. 1d, upper panels), whereas Hel-v1 was expressed only in limited cases of ATL (Fig. 1d, lower panels). In four cases, Helios was not expressed. Collectively, our mRNA analysis showed that Helios expression was generally deregulated in ATL cells.

Genomic abnormalities at the *Helios* locus in primary ATL cells. To investigate the *Helios* locus in ATL, we retrieved data from our gene copy number analysis[3] and found that specific genomic deletion was accumulated at the *Helios* locus in ATL samples (17/168 cases, Fig. 2). All 17 cases were aggressive-type ATL (12/17 lymphoma types and 5/17 acute types). Furthermore, we found that two acute ATL cases in Figure 1(a) (#9 and #14), which showed severely deregulated or lost Helios expression, had a genomic deletion of the *Helios* locus.

Dimerization ability of ATL-type Helios isoforms with wild-type Helios or Ikaros. Consistent with a previously published report,[33] co-immunoprecipitation analyses confirmed that wild-type Hel-1 formed homodimers with themselves and heterodimers with wild-type Ikaros (Ik-1) protein (Fig. 3a, top panel, lane 1 and lane 4). In contrast, the dimerization activity of another artificial Helios mutant (Hel-ΔC), which lacks the dimerization domain at the C-terminal region, was dramatically declined (Fig. 3b, top panel, lane 1 and lane 4). We confirmed that all ATL-type Helios proteins could interact with Hel-1 and Ik-1, despite the fact that all of them lack various sets of the N-terminal exons (Fig. 3c–f).

Cytoplasmic localization of ATL-type Helios isoforms lacking exon 6. Ectopically expressed Hel-1 and Ik-1 were localized in the nucleus (Fig. 4a, top two panels). Regarding the ATL-type Helios isoforms, we found that Hel-5 and Hel-v1 were localized in the nucleus, whereas Hel-6 and Hel-v2, both of which lack exon 6, were substantially localized in the cytoplasm (Fig. 4a, middle four panels). We also confirmed the cytoplasmic localization of Hel-Δexon 6, which is an artificial Helios mutant lacking only exon 6 (Fig. 4a, bottom panel). Thus, exon 6 appears to be critical for nuclear localization of Helios proteins. Furthermore, defect of exon 6 led to disruption of the

Fig. 1. (On the next page) Abnormal expression of Helios mRNA in primary adult T-cell leukemia (ATL) cells. (a) Expression analysis of Ikaros family genes in PBMCs by full-length RT-PCR (Acute, $n = 22$; Chronic, $n = 10$; Smoldering, $n = 5$; HTLV-1 carriers, $n = 5$; High-risk carriers, $n = 4$). To detect and distinguish alternative splicing variants, PCR analyses were carried out with the sense and antisense primer sets designed in the first and final exons of each full-length transcript of Ikaros family genes. Obtained cDNAs were cloned and their sequences were analyzed. The samples acute #4, 4′, and 4″ were derived from the same patient, but were studied independently. (b) Expression of Ikaros family genes in PBMCs from normal volunteers ($n = 10$). (c) Schematic representation of Hel-1, Hel-2, and ATL-type Helios isoforms identified in this study. Hel-variant 1 (Hel-v1) and Hel-variant 2 (Hel-v2) are novel isoforms in ATL. Arrows indicate primer locations of full-length PCR for Helios. Ex, exon; F1–F6, functional zinc-finger domains. (d) Nested PCR with specific primer sets, which were designed at exon junction of exon 1–5 or exon 2–5 for detection of Hel-5 and Hel-6 (upper panel), or detection of Hel-v1 (lower panel), respectively. Arrows indicate primer locations.

doi: 10.1111/cas.12181

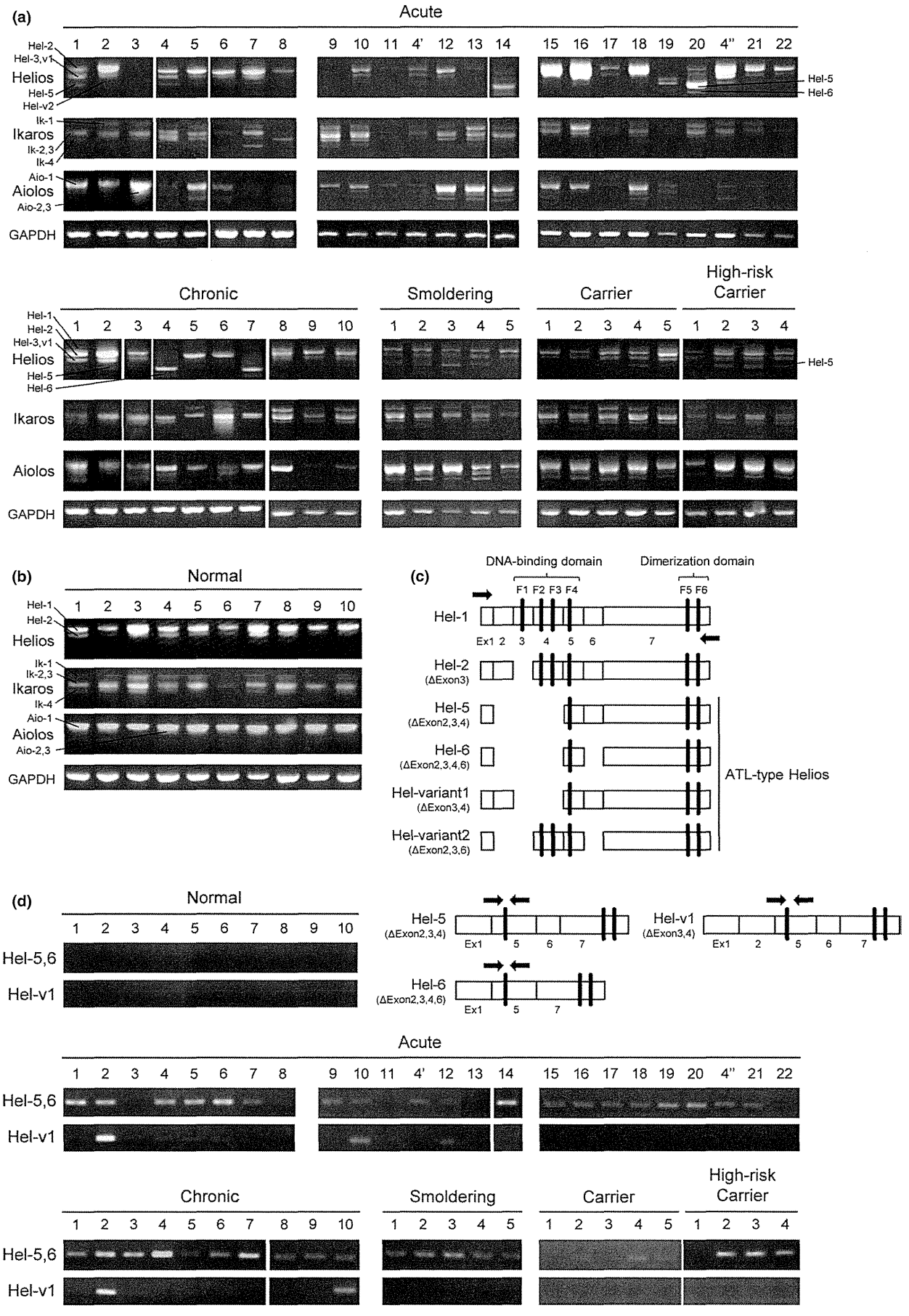

cellular localization of binding partners. When Hel-6 or Hel-v2 were co-expressed with Hel-1 or Ik-1, they were co-localized in the cytoplasm (Fig. 4b, Fig. S2).

Dominant-negative function of ATL-type Helios isoforms against wild-type Helios and Ikaros. We next examined the functional aspects of these ATL-type Helios isoforms by evaluating their DNA-binding capacities. For EMSA, we used an oligonucleotide probe derived from the promoter region of human *Hes1*, which was a direct target of Ikaros.[34,35] Ectopically expressed Hel-1 or Ik-1 could bind human *Hes1* promoter DNA (Fig. 5a). Supershift assays confirmed the binding specificity (Fig. 5b). In contrast, all ATL-type Helios isoforms did not show any specific binding to the *Hes1* promoter (Fig. 5a). This impossibility of specific DNA binding of ATL-type Helios was confirmed with another independent DNA probe, IkBS4[33,36] (data not shown). In addition, it was found in co-expression experiments that Hel-5 had antagonistic effects on the DNA binding capacity of Ik-1 in a dose-dependent manner (Fig. 5c). Reporter assays showed that Hel-1 and Ik-1 suppressed *Hes1* promoter activity. However, ATL-type Helios isoforms did not show any suppressive activity, and actually slightly activated the promoter (Fig. 5d). Furthermore, they also inhibited the suppressive function of Hel-1 and Ik-1 in a dose-dependent manner (Fig. 5e, Fig. S3). These data clearly indicate that ATL-type Helios isoforms are functionally defective because of a DNA binding deficiency and act dominant-negatively in transcriptional suppression induced by Hel-1 or Ik-1. We also confirmed that Hel-2, which lacks only exon 3 and is a major isoform in ATL cells, did not possess suppressive activity against *Hes1* promoter in spite of having binding activity (Fig. 5a,d).

Major ATL-type Helios variant, Hel-5, promotes T cell growth. Given the tumor-suppressive roles of Ikaros family members,[12–15] it was expected that abnormal splicing of Helios could contribute to T cell leukemogenesis. The mRNA level of Helios was significantly downregulated in ATL-related cell lines compared with that in T-cell lines without HTLV-1 (Fig. 6a, Fig. S4). Moreover, Helios protein was not detected in any ATL-derived or HTLV-1-infected cell lines used in this study (Fig. 6b). In contrast, the expression levels of Ikaros mRNA did not show major differences between HTLV-1-infected and uninfected T-cell lines. Those of Aiolos were low in most cell lines irrespective of HTLV-1 infection (Fig. 6a, Fig. S4). Ikaros protein was detected in all T-cell lines used in this study (Fig. 6b). To elucidate the cellular effects of the expression of dominant-negative ATL-type Helios isoforms in T cells, we established stable Jurkat cells expressing Hel-5 (Fig. 6c). A cell proliferation assay confirmed that Hel-5 expression significantly promoted Jurkat cell proliferation

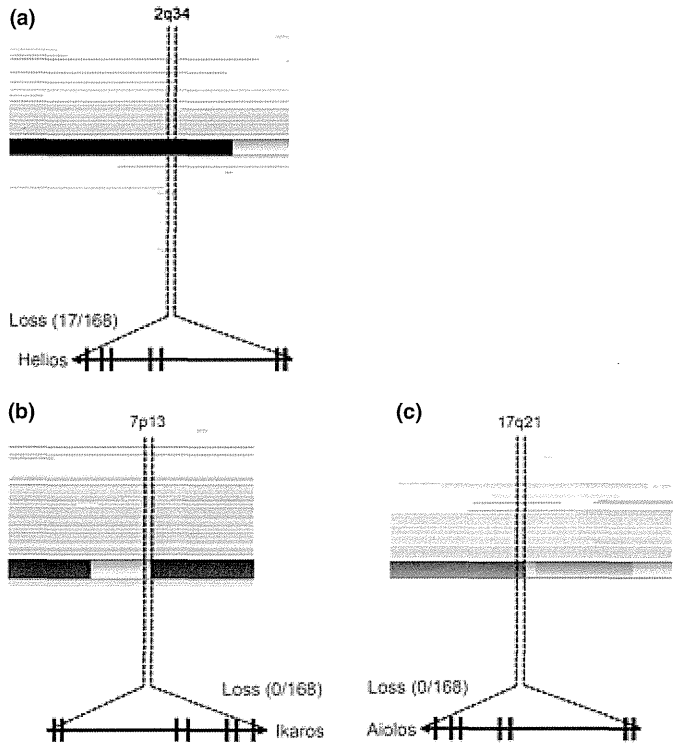

Fig. 2. Genetic abnormalities in *Helios* locus in primary adult T-cell leukemia cells. The results of our copy number analyses[3] (total number, $n = 168$; acute type, $n = 35$; chronic type, $n = 41$; lymphoma type, $n = 44$; smoldering type, $n = 10$; intermediate, $n = 1$; unknown diagnosis, $n = 37$). Tumor-associated deletion of *Helios* region (17/168) was detected (a). No specific genomic losses were observed in *Ikaros* (b) or *Aiolos* loci (c). Recurrent genetic changes are depicted by horizontal lines based on Copy Number Analyser for GeneChip output of the single nucleotide polymorphism array analysis.

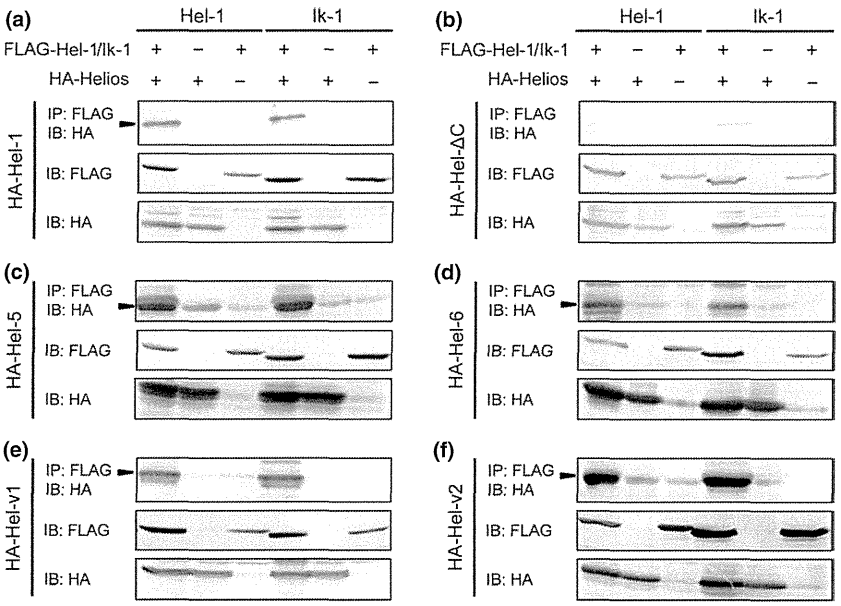

Fig. 3. Dimerization ability of adult T-cell leukemia (ATL)-type Helios isoforms. *In vitro* dimerization assays by co-immunoprecipitation between ATL-type Helios and wild-type Helios or Ikaros proteins. 293T cells were transfected with the indicated combination of expression vectors and subjected to co-immunoprecipitation analyses (top panels). Arrowheads indicate the complex of FLAG and HA-tagged proteins. Middle and bottom panels show the input samples. Hel-1 (a) and Hel-ΔC (b) included as positive and negative controls, respectively. ATL-specific isoforms, Hel-5 (c), Hel-6 (d), Hel-v1 (e), and Hel-v2 (f) were tested. IB, immunoblot; IP, immunoprecipitant.

doi: 10.1111/cas.12181

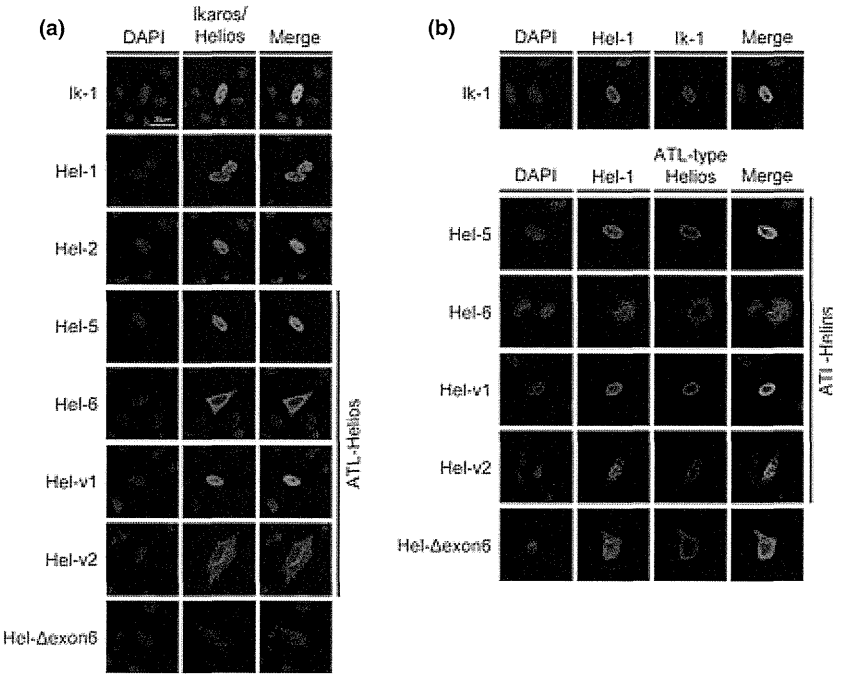

Fig. 4. Subcellular localization of adult T-cell leukemia (ATL)-type Helios isoforms. Immunostaining analyses of Helios and Ikaros proteins. HeLa cells were transfected with each individual expression vector (a) or the indicated combination of expression vectors (b). Each protein was visualized with anti-FLAG (green) or anti-HA antibodies (red). Nuclei were detected by DAPI staining (blue). Colocalization between Ik-1 and ATL-type Helios was shown in Fig. S2. Hel-v1, Hel-variant 1; Hel-v2, Hel-variant 2.

(Fig. 6d). To examine whether the cellular effect of Hel-5 was due to its dominant-negative function against Hel-1 and Ik-1, we carried out further knockdown analyses with specific shRNAs (Fig. 6e). The results showed that knockdown of wild-type Helios or Ikaros led to enhanced cell growth (Fig. 6f), which was consistent with the results of enforced Hel-5 expression. These results collectively suggested that counteraction of Ikaros or Helios by dominant-negative isoforms contributed to T cell growth.

Helios deficiency causes expression of various genes in T cells. We globally searched mRNA expression changes using microarray analysis of Jurkat cells expressing Hel-5 and those of knocked-down Helios or Ikaros (Fig. 7a,b). The results clearly showed differentially expressed gene sets between the transformants and control cells (Fig. 7c). Furthermore, pathway analysis[37] of each upregulated gene set identified activation of several signaling cascades. In particular, we focused on six common pathways identified in both Hel-5 transduced and Helios or Ikaros knocked-down Jurkat cells (Fig. 7d). These pathways are important for various T cell regulations, for example, cell growth, apoptosis resistance, and migration activity. Among these pathways, it has not been reported that the shingosine-1-phosphate (S1P) pathway is regulated by the Ikaros family. We confirmed overexpressed *S1PR1* and *S1PR3*, which are critical receptors for the activation of the S1P pathway, in manipulated Jurkat samples (Fig. 7e).

Discussion

In the present study, on the basis of the integrated analysis of ATL cells using our biomaterial bank in Japan, we revealed a novel molecular characteristic of ATL cells, which is a profound abnormality in the expression of Helios. The abnormal alternative splicing and, in some cases, loss of Helios expression appear to be a part of the basis for advantageous cell growth and survival in ATL cells. We also showed the tumor-suppressive function and target genes, as well as pathways of Helios, in mature human T cells.

Characterization of Ikaros family members revealed profound abnormalities in Helios expression in ATL cells: (i) biased and increased expression of alternatively spliced variants; (ii) suppression of Hel-1 expression; (iii) lack of Helios expression in some cases; and (iv) frequent genomic defects of the *Helios* locus. Our results also revealed that alternatively spliced Helios variants are expressed in PBMCs of HTLV-1 carriers, suggesting that the abnormal splicing of Helios may occur in HTLV-1-infected cells at the carrier state until progression to leukemia development. However, the genomic deletions appear to be one of the important genetic events during the latter stages of leukemia development, as they were observed only in aggressive subtypes of ATL.

The structural characteristics of the ATL-type Helios variants involve a selective lack of one or more zinc fingers in the N-terminal domain. The results of this study indicated that these variant proteins lost DNA binding activity, whereas the capacity of dimerization was preserved. Therefore, these variant proteins hindered transcriptional activities of Ikaros family proteins, showing dominant-negative effects. In addition, a part of ATL-type Helios isoform, which lacks exon 6, is linked to abnormal localization of wild-type Helios and Ikaros. We confirmed that Helios isoforms lacking exon 6 were overexpressed in primary ATL cells (Fig. S5). Interestingly, Hel-2 has reduced transcriptional suppressive activity compared with Hel-1, although it can bind to the target sequence as well as Hel-1. This is similar to a previous report,[36] which noted that the activity of mouse Ik-2 protein for the reporter gene was remarkably lower than that of Ik-1, whereas the binding affinities of Ik-1 and Ik-2 were similar. The exon 3 skip occurred more frequently in ATL cells, compared to PBMCs from normal volunteers (Fig. S6). These results collectively indicate that all abnormalities of Helios expression, including loss of or decreased Hel-1 expression and upregulated Hel-2 and ATL-type Helios, result in abrogation of Ikaros family functions in ATL cells.

We also confirmed that *Hes1*, a target gene of the Notch pathway, is one of the targets of Helios as well as Ikaros.[34,35] A recent study reported that activated Notch signaling may be important to ATL pathogenesis and that Hes1 is upregulated in ATL cells.[38] Thus, we examined expression levels of Hes1 mRNA by quantitative RT-PCR and confirmed the

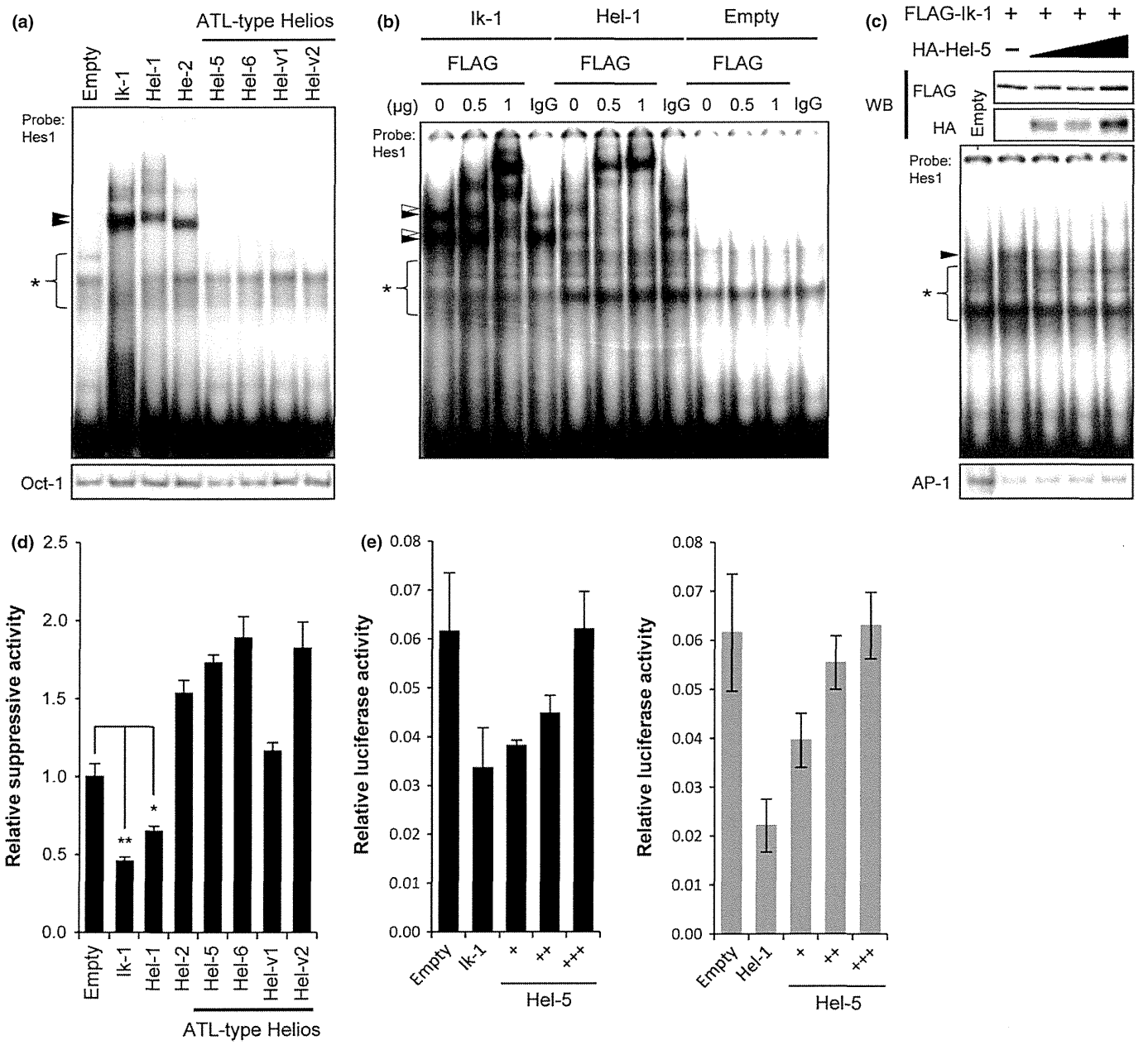

Fig. 5. Dominant-negative function of adult T-cell leukemia (ATL)-type Helios isoforms. (a) DNA-binding activities of wild-type Helios or Ikaros and ATL-type Helios proteins. Each FLAG-tagged Helios or Ikaros isoforms were ectopically expressed in 293T cells and their nuclear extracts were subjected to EMSA with a [γ-^{32}P]-labeled *Hes1* promoter probe. Oct-1 probe was used as an internal control. Arrowheads indicate Helios or Ikaros complexes. *Non-specific bands. Hel-v1, Hel-variant 1; Hel-v2, Hel-variant 2. (b) Results of supershift assays. Anti-FLAG (0, 0.5, 1 μg) or control IgG (1 μg) antibodies were added to each nuclear extract prior to electrophoresis. The black and white arrowheads indicate the supershifted bands of Ik-1 and Hel-1, respectively. (c) Antagonistic effects of Hel-5 on DNA-binding of Ik-1 tested by EMSA. The molar ratios of Ik-1 to Hel-5 plasmids are 1:1, 1:4, and 1:8. Expression levels of FLAG-Ik-1 and HA-Hel-5 were assessed by immunoblotting. The arrowheads indicate the Ik-1 specific band. AP-1 probe was used as an internal control. WB, western blot. (d) Transcriptional suppression activities of various Helios or Ikaros isoforms tested by *Hes1* promoter-luciferase reporter systems (n = 3, mean ± SD). Basal *Hes1* promoter activity was defined as firefly/renilla ratio, and suppression activities of Helios or Ikaros are relatively presented. Statistical significance was evaluated by unpaired Student's t-test (*P < 0.05; **P < 0.01). (e) Inhibitory function of Hel-5 against Ik-1 and Hel-1 tested by *Hes1* promoter assay (n = 3, mean ± SD). The molar ratios of Ik-1 or Hel-1 to Hel-5 plasmids are 1:1, 1:2, and 1:3. Relative luciferase activities were defined as firefly/renilla ratio.

upregulation in our ATL samples (Fig. S7). Hes1 has been reported to directly promote cell proliferation through the transcriptional repression of p27kip1.[39] Taken together, our results suggest a possibility that abnormalities in Helios expression are one of the causes of Hes1 activation, which may be one of the genetic events involved in ATL leukemogenesis.

Our results show that the Hel-5 variant may have an oncogenic role, whereas the wild-type Helios, Hel-1, shows tumor suppressor-like activity. These findings are consistent with previous findings in mice.[15] Furthermore, our description of expression profiles of stable cells followed by pathway analyses showed activation of several important pathways in lymphocytes for the regulation of proliferation, survival, and others. In particular, we discovered novel molecular cross-talk between the Ikaros family and the S1P pathway. The S1P–S1PR1 axis is known to play important

doi: 10.1111/cas.12181

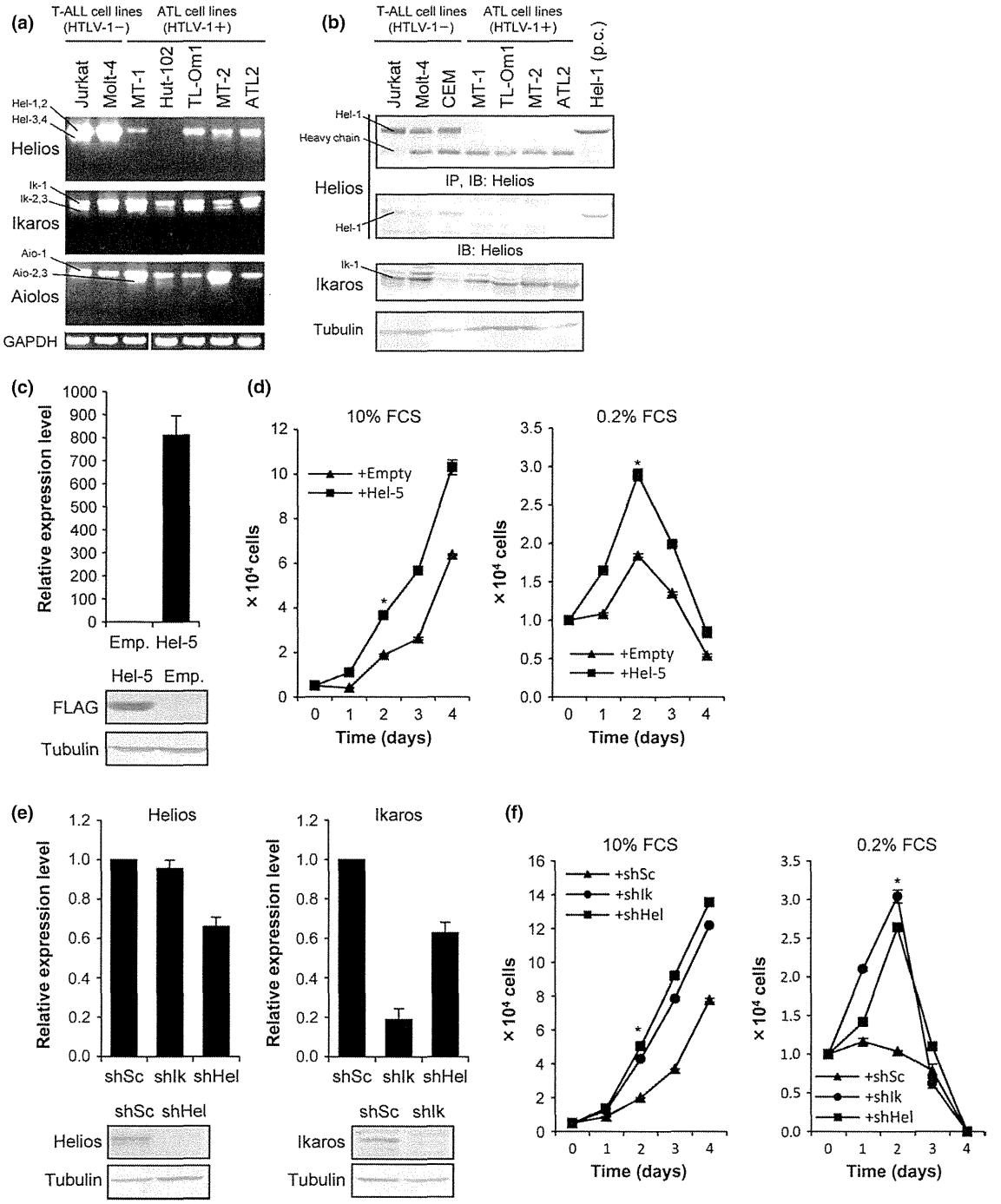

Fig. 6. Hel-5 functions in T cell growth and survival. (a) Expression patterns and levels of Ikaros family genes in various cell lines examined by RT-PCR. ATL, adult T-cell leukemia; T-ALL, acute T lymphoblastic leukemia. (b) Results of immunoblotting analyses of the immunoprecipitants (top panel) and cell lysates (lower panels). Positive control (p.c.), Hel-1 transfectant. IB, immunoblot; IP, immunoprecipitant. (c) Establishment of Jurkat cells stably expressing Hel-5. The Hel-5 level was quantified by quantitative RT-PCR (top, $n = 3$, mean ± SD) and immunoblotting (bottom). (d) Cell proliferation analysis of control cells (▲) and Hel-5-expressing Jurkat cells (■) under two FCS conditions ($n = 3$, mean ± SD). Statistical significance was observed (*P <0.01, Student's t-test). (e) Knockdown analyses of Helios or Ikaros in Jurkat cells. The Helios and Ikaros levels were evaluated by quantitative RT-PCR (top, $n = 3$, mean ± SD) and immunoblotting (bottom), respectively. (f) Cell proliferation curves of scrambled shRNA (shSc) cells (▲), shIkaros (shIk) cells (●), and shHelios (shHel) cells (■) were examined in two FBS conditions ($n = 3$, mean ± SD; *$P < 0.01$).

roles in regulation of the immune system, apoptosis, cell cycle, and migration of lymphocytes.[40–42] Recently, activation of the S1P pathway in various diseases, including leukemia, has been reported, and the therapeutic potential of S1PR1 inhibitors was suggested.[42] Studies of functional roles of S1P pathway activation in ATL cells are now underway in our laboratory.

In conclusion, our present study revealed a novel aspect of molecular abnormalities in ATL cells: a profound deregulation in Helios expression, which appears to play an important role in T-cell proliferation. Our experimental approaches also imply that, in addition to genetic and epigenetic abnormalities, ATL shows abnormal splicing, which has been observed in various human diseases including cancers.[43–45]

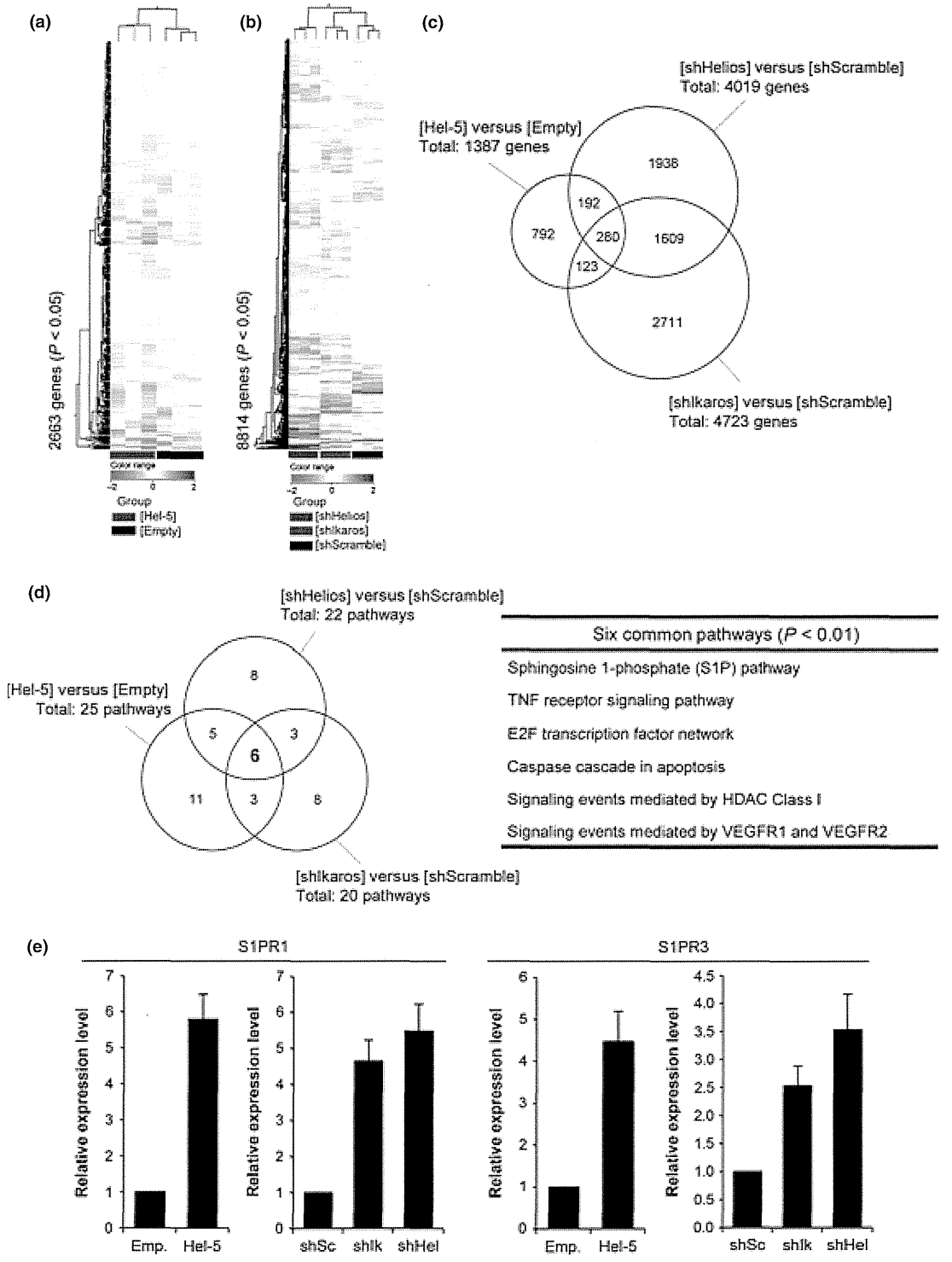

Fig. 7. Comprehensive search for Helios target genes by microarray analysis. (a,b) Gene expression analysis of Jurkat stable cells. The gene expression patterns of Jurkat cells expressing Hel-5 (n = 3), shIkaros (n = 3), and shHelios (n = 3) were comprehensively analyzed by microarray technique. The obtained 2D hierarchical clusters and Pearson's correlation between the cells expressing Hel-5 or not (a) and the cells introducing shHel, shIk, or shSc (b). (c) Venn diagram of differential gene expression pattern in the Jurkat sublines. The each differential expression gene set (5-fold changes, $P < 1 \times 10^{-5}$) was compared. (d) Venn diagram depicting the overlap between the outputs of pathway analysis in Jurkat sublines. The analysis was based on the NCI-Nature Pathway Interaction Database.[37] Each differential pathway set (t-test, $P < 0.01$) was compared and the common pathways listed. (e) Results of quantitative RT-PCR of shingosine-1-phosphate receptor 1 (S1PR1) and receptor 3 (S1PR3) in Jurkat sublines (n = 3, mean ± SD). HDAC, histone deacetylase; VEGFR, vascular endothelial growth factor receptor.

Acknowledgments

We thank Mr. M. Nakashima and Ms. T. Akashi for support and maintenance of the Joint Study on Prognostic Factors of ATL Development. This work is supported by JSPS KAKENHI Grant Numbers 24790436 (M.Y.), 23390250 (T.W.), 23659484 (T.W.), 23 6291 (S.A.), NEXT KAKENHI Grant Number 221S0001 (T.W.), and a Grant-in-Aid from the Ministry of Health, Labor and Welfare of Japan H24-G-004 (M.Y. and T.W.).

doi: 10.1111/cas.12181

Disclosure Statement

The authors have no conflict of interest.

References

1 Yamaguchi K, Watanabe T. Human T lymphotropic virus type-I and adult T-cell leukemia in Japan. *Int J Hematol* 2002; **76**: 240–45.
2 Iwanaga M, Watanabe T, Utsunomiya A *et al.* Human T-cell leukemia virus type I (HTLV-1) proviral load and disease progression in asymptomatic HTLV-1 carriers: a nationwide prospective study in Japan. *Blood* 2010; **116**: 1211–19.
3 Yamagishi M, Nakano K, Miyake A *et al.* Polycomb-mediated loss of miR-31 activates NIK-dependent NF-κB pathway in adult T cell leukemia and other cancers. *Cancer Cell* 2012; **21**: 121–35.
4 Yamagishi M, Watanabe T. Molecular hallmarks of adult T cell leukemia. *Front Microbiol* 2012; **3**: 334.
5 Lo K, Landau NR, Smale ST. LyF-1, a transcriptional regulator that interacts with a novel class of promoters for lymphocyte-specific genes. *Mol Cell Biol* 1991; **11**: 5229–43.
6 Georgopoulos K, Moore DD, Derfler B. Ikaros, an early lymphoid-specific-transcription factor and a putative mediator for T cell commitment. *Science* 1992; **258**: 808–12.
7 Hahm K, Ernst P, Lo K, Kim GS, Turck C, Smale ST. The lymphoid transcription factor LyF-1 is encoded by specific, alternatively spliced mRNAs derived from the Ikaros gene. *Mol Cell Biol* 1994; **14**: 7111–23.
8 Sun L, Liu A. Zinc finger-mediated protein interactions modulate Ikaros activity, a molecular control of lymphocyte development. *EMBO J* 1996; **15**: 5358–69.
9 Morgan B, Sun L, Avitahl N *et al.* Aiolos, a lymphoid restricted transcription factor that interacts with Ikaros to regulate lymphocyte differentiation. *EMBO J* 1997; **16**: 2004–13.
10 Kelley CM, Ikeda T, Koipally J *et al.* Helios, a novel dimerization partner of Ikaros expressed in the earliest hematopoietic progenitors. *Curr Biol* 1998; **8**: 508–15.
11 Cobb BS, McCarty AS, Brown KE *et al.* Helios, a T cell-restricted Ikaros family member that quantitatively associates with Ikaros at centromeric heterochromatin. *Genes Dev* 1998; **12**: 782–96.
12 Winandy S, Wu P, Georgopoulos K. A dominant mutation in the Ikaros gene leads to rapid development of leukemia and lymphoma. *Cell* 1995; **83**: 289–99.
13 Wang JH, Nichogiannopoulou A, Wu L *et al.* Selective defects in the development of the fetal and adult lymphoid system in mice with an Ikaros null mutation. *Immunity* 1996; **5**: 537–49.
14 Wang JH, Avitahl N, Cariappa A *et al.* Aiolos regulates B cell activation and maturation to effector state. *Immunity* 1998; **9**: 543–53.
15 Zhang Z, Swindle CS, Bates JT, Ko R, Cotta CV, Klug CA. Expression of a non-DNA-binding isoform of Helios induces T-cell lymphoma in mice. *Blood* 2007; **109**: 2190–7.
16 Sun L, Crotty ML, Sensel M *et al.* Expression of dominant-negative Ikaros isoforms in T-cell acute lymphoblastic leukemia. *Clin Cancer Res* 1999; **5**: 2112–20.
17 Nakase K, Ishimaru F, Avitahl N *et al.* Dominant negative isoform of the Ikaros gene in patients with adult B-cell acute lymphoblastic leukemia. *Cancer Res* 2000; **60**: 062–4065.
18 Takanashi M, Yagi T, Imamura T *et al.* Expression of the Ikaros gene family in childhood acute lymphoblastic leukaemia. *Br J Haematol* 2002; **117**: 525–30.
19 Nishii K, Katayama N, Miwa H. Non-DNA-binding Ikaros isoform gene expressed in adult B-precursor acute lymphoblastic leukemia. *Leukemia* 2002; **16**: 1285–92.
20 Tonnelle C, Imbert M-C, Sainty D, Granjeaud S, N'Guyen C, Chabannon C. Overexpression of dominant-negative Ikaros 6 protein is restricted to a subset of B common adult acute lymphoblastic leukemias that express high levels of the CD34 antigen. *Hematol J* 2003; **4**: 104–9.
21 Klein F, Feldhahn N, Herzog S *et al.* BCR-ABL1 induces aberrant splicing of IKAROS and lineage infidelity in pre-B lymphoblastic leukemia cells. *Oncogene* 2006; **25**: 1118–24.
22 Zhou F, Mei H, Jin R, Li X, Chen X. Expression of ikaros isoform 6 in chinese children with acute lymphoblastic leukemia. *J Pediatr Hematol Oncol* 2011; **33**: 429–32.
23 Mullighan CG, Miller CB, Radtke I *et al.* BCR-ABL1 lymphoblastic leukaemia is characterized by the deletion of Ikaros. *Nature* 2008; **453**: 110–14.
24 Kano G, Morimoto A, Takanashi M *et al.* Ikaros dominant negative isoform (Ik6) induces IL-3-independent survival of murine pro-B lymphocytes by activating JAK-STAT and up-regulating Bcl-xl levels. *Leuk Lymphoma* 2008; **49**: 965–73.
25 Iacobucci I, Lonetti A, Messa F *et al.* Expression of spliced oncogenic Ikaros isoforms in Philadelphia-positive acute lymphoblastic leukemia patients treated with tyrosine kinase inhibitors: implications for a new mechanism of resistance. *Blood* 2008; **112**: 3847–55.
26 Mullighan CG, Su X, Zhang J *et al.* Deletion of IKZF1 and prognosis in acute lymphoblastic leukemia. *N Engl J Med* 2009; **360**: 470–80.
27 Kuiper RP, Waanders E, van der Velden VHJ *et al.* IKZF1 deletions predict relapse in uniformly treated pediatric precursor B-ALL. *Leukemia* 2010; **24**: 1258–64.
28 Nakase K, Ishimaru F, Fujii K *et al.* Overexpression of novel short isoforms of Helios in a patient with T-cell acute lymphoblastic leukemia. *Exp Hematol* 2002; **30**: 313–17.
29 Fujii K, Ishimaru F, Tabayashi T *et al.* Over-expression of short isoforms of Helios in patients with adult T-cell leukaemia/lymphoma. *Br J Haematol* 2003; **120**: 986–9.
30 Fujiwara SI, Yamashita Y, Nakamura N *et al.* High-resolution analysis of chromosome copy number alterations in angioimmunoblastic T-cell lymphoma and peripheral T-cell lymphoma, unspecified, with single nucleotide polymorphism-typing microarrays. *Leukemia* 2008; **22**: 1891–8.
31 Fujimoto R, Ozawa T, Itoyama T, Sadamori N, Kurosawa N, Isobe M. HELIOS-BCL11B fusion gene involvement in a t(2;14)(q34;q32) in an adult T-cell leukemia patient. *Cancer Genet* 2012; **205**: 356–64.
32 Shimoyama M. Diagnostic criteria and classification of clinical subtypes of adult T-cell leukaemia-lymphoma. A report from the Lymphoma Study Group (1984–87). *Br J Haematol* 1991; **79**: 428–37.
33 Tabayashi T, Ishimaru F, Takata M *et al.* Characterization of the short isoform of Helios overexpressed in patients with T-cell malignancies. *Cancer Sci* 2007; **98**: 182–8.
34 Kathrein KL, Chari S, Winandy S. Ikaros directly represses the notch target gene Hes1 in a leukemia T cell line: implications for CD4 regulation. *J Biol Chem* 2008; **283**: 10476–84.
35 Kleinmann E, Geimer Le Lay AS, Sellars M, Kastner P, Chan S. Ikaros represses the transcriptional response to Notch signaling in T-cell development. *Mol Cell Biol* 2008; **28**: 7465–75.
36 Molnár A, Georgopoulos K. The Ikaros gene encodes a family of functionally diverse zinc finger DNA-binding proteins. *Mol Cell Biol* 1994; **14**: 8292–303.
37 Schaefer CF, Anthony K, Krupa S *et al.* PID: the pathway interaction database. *Nucleic Acids Res* 2009; **37**: D674–9.
38 Pancewicz J, Taylor JM, Datta A. Notch signaling contributes to proliferation and tumor formation of human T-cell leukemia virus type 1-associated adult T-cell leukemia. *Proc Natl Acad Sci USA* 2010; **107**: 16619–24.
39 Murata K, Hattori M, Hirai N *et al.* Hes1 directly controls cell proliferation through the transcriptional repression of p27Kip1. *Mol Cell Biol* 2005; **25**: 4262–71.
40 Maeda Y, Seki N, Sato N, Sugahara K, Chiba K. Sphingosine 1-phosphate receptor type 1 regulates egress of mature T cells from mouse bone marrow. *Int Immunol* 2010; **22**: 515–25.
41 Spiegel S, Milstien S. The outs and the ins of sphingosine-1-phosphate in immunity. *Nat Rev Immunol* 2011; **11**: 403–15.
42 Maceyka M, Harikumar KB, Milstien S, Spiegel S. Sphingosine-1-phosphate signaling and its role in disease. *Trends Cell Biol* 2012; **22**: 50–60.
43 Ghigna C, Valacca C, Biamonti G. Alternative splicing and tumor progression. *Curr Genomics* 2008; **9**: 556–70.
44 David CJ, Manley JL. Alternative pre-mRNA splicing regulation in cancer: pathways and programs unhinged. *Genes Dev* 2010; **24**: 2343–64.
45 Blair CA, Zi X. Potential molecular targeting of splice variants for cancer treatment. *Indian J Exp Biol* 2011; **49**: 836–9.

Supporting Information

Additional Supporting Information may be found in the online version of this article:

Fig. S1. Deregulated expression of Ikaros family genes in primary adult T-cell leukemia cells.

Fig. S2. Colocalization of wild-type Ikaros and adult T-cell leukemia-type Helios.

Fig. S3. Dominant-negative inhibition of Hel-6, Hel-v1, and Hel-v2 in the suppressive activities of wild-type Helios and Ikaros.

Fig. S4. Downregulation of the expression of Helios mRNA in HTLV-1-positive T cell lines.

Fig. S5. Overexpression of abnormal Helios isoforms lacking exon 6 in adult T-cell leukemia samples.

Fig. S6. Relative value of Helios transcripts skipping exon 3 to all is upregulated in primary adult T-cell leukemia cells.

Fig. S7. Upregulated expression of Hes1 in primary adult T-cell leukemia cells.

Table S1. Clinical characteristics of adult T-cell leukemia patients and HTLV-1 carriers.

Table S2. Primer list and probe sequences.

doi: 10.1111/cas.12181

THE PROTEIN SOCIETY

Mutations for decreasing the immunogenicity and maintaining the function of core streptavidin

Kyohei Yumura,[1,2] Mihoko Ui,[2] Hirofumi Doi,[3] Takao Hamakubo,[3] Tatsuhiko Kodama,[3] Kouhei Tsumoto,[1,2]* and Akira Sugiyama[3]*

[1]Institute of Medical Science, The University of Tokyo, Minato-ku, Tokyo 108-8639, Japan

[2]Department of Medical Genome Sciences, Graduate School of Frontier Sciences, The University of Tokyo, Kashiwa 277-8562, Japan

[3]Research Center for Advanced Science and Technology, The University of Tokyo, Komaba, Tokyo 153-8904, Japan

Received 15 September 2012; Revised 24 November 2012; Accepted 26 November 2012
DOI: 10.1002/pro.2203
Published online 6 December 2012 proteinscience.org

Abstract: The defining property of core streptavidin (cSA) is not only its high binding affinity for biotin but also its pronounced thermal and chemical stability. Although potential applications of these properties including therapeutic methods have prompted much biological research, the high immunogenicity of this bacterial protein is a key obstacle to its clinical use. To this end, we have successfully constructed hypoimmunogenic cSA muteins in a previous report. However, the effects of these mutations on the physicochemical properties of muteins were still unclear. These mutations retained the similar electrostatic charges to those of wild-type (WT) cSA, and functional moieties with similar hydrogen bond pattern. Herein, we performed isothermal titration calorimetry, differential scanning calorimetry, and sodium dodecyl sulfate–polyacrylamide gel electrophoresis to gain insight into the physicochemical properties and functions of these modified versions of cSA. The results indicated that the hypoimmunogenic muteins retained the biotin-binding function and the tetramer structure of WT cSA. In addition, we discuss the potential mechanisms underlying the success of these mutations in achieving both immune evasion and retention of function; these mechanisms might be incorporated into a new strategy for constructing hypoimmunogenic proteins.

Keywords: streptavidin; low immunogenicity; protein engineering; thermodynamic analysis; isothermal titration calorimetry; differential scanning calorimetry; therapeutic protein

Introduction

Core streptavidin (cSA), a protein from *Streptomyces avidinii*, is well known to have an extremely strong binding affinity to biotin ($K_D \sim 10^{-14}$M).[1,2] cSA is also highly resistant to heat,[3,4] denaturants,[5] and proteolysis.[6,7] Because of its unique properties, cSA has been put to practical use in various areas, including biochemistry,[8] and shows therapeutic potential. One possible therapeutic use is in a pretargeting system for drug delivery.[9] However, the immunogenicity of this bacteria-derived protein is an obstacle to its clinical

Abbreviations: cSA, core streptavidin; DSC, differential scanning calorimetry; FFF-MALS, field-flow fractionation–multiangle light scattering; ITC, isothermal titration calorimetry; SDS–PAGE, sodium dodecyl sulfate–polyacrylamide gel electrophoresis; WT, wild-type.

Additional Supporting Information may be found in the online version of this article.

Grant sponsors: World-Leading Innovative R&D on Science and Technology (FIRST) of the Japan Society for the Promotion of Science (Funding program); Grant sponsor: Ministry of Education, Science, Sports, and Culture of Japan (Promotion of Science and by Grants-in-Aid for General Research, K.T.).

*Correspondence to: Kouhei Tsumoto, Institute of Medical Science, Transmittal form, The University of Tokyo, Minato-ku, Tokyo 108-8639, Japan. E-mail: tsumoto@ims.u-tokyo.ac.jp or Akira Sugiyama. E-mail: sugiyama@lsbm.org

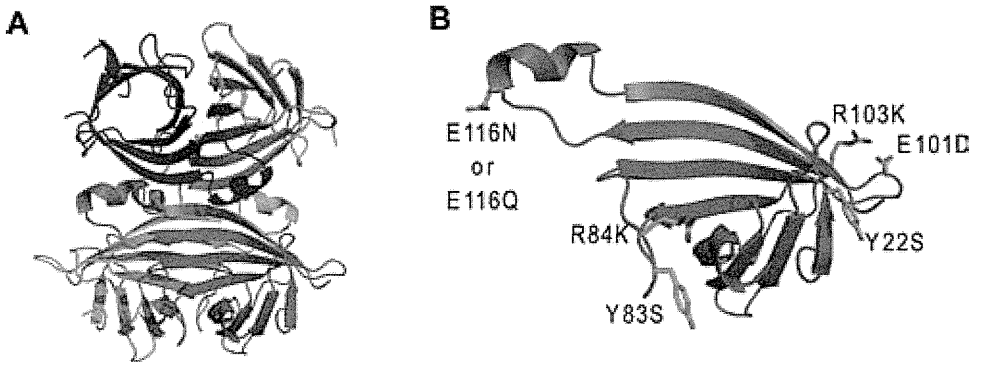

Figure 1. The crystal structure and mutated residues of cSA. (A) Tetrameric structure of cSA WT (from Ref. 20). (B) Mutated residues are indicated as stick forms in a monomeric subunit. All mutations were induced at surface residues not directly involved in either biotin binding or tetramerization.

application.[10–12] One of the most successful approaches for reducing immunogenicity[13,14] is that used for humanizing antibodies.[15] Although grafting sequences from the human homolog into a target protein can reduce the immunogenicity of the resulting hybrid molecule, this strategy cannot be applied to cSA because its human counterpart has not yet been found.

Site-directed mutagenesis is another strategy for reducing the immunogenicity of nonhuman proteins.[16,17] Previous reports have suggested that the immunogenicity of nonhuman proteins was decreased through the elimination of charged or aromatic residues on B-cell epitopes by the replacement of these residues mainly with alanine.[16,17] This mutagenesis strategy has been applied successfully to cSA.[18] Because charged and aromatic residues on the protein surface are considered to be important for immune recognition of proteins including cSA, these residues not directly involved in biotin binding or tetramerization were mutated.[18] This method diminished the immunoreactivity of the mutated cSA to murine and human antistreptavidins, because some of these mutations, especially those at Y83, involved key epitopes for immune recognition.[16] However, the mutations also increased the dissociation rate from biotin,[16] suggesting that the biotin-binding function was reduced. The relationship between the structure and function of cSA seems to be strict,[19] and some mutations reportedly have led to dimerization, destabilization, and decreased binding activity of cSA.[19] Therefore, strategies for mutagenesis of cSA should be considered carefully in regard to both the target residues and those to be substituted.

We also previously performed site-directed mutagenesis of various charged and aromatic residues of cSA that were proposed to be involved in its immune recognition (Fig. 1)[20] and designed the hypoimmunogenic muteins. The immunoreactivities of these muteins against crab-eating monkey antiserum were evaluated by surface plasmon resonance (Table I and Supporting Information Fig. S1).[21,22] The immunogenicity analyses about T-cell epitope were performed *in silico* model (Supporting Information Table S1).[22–25] Some muteins had exceedingly low immunoreactivities and the number of T-cell epitope was decreased. However, the effects of these mutations on the physicochemical properties and functions of the resulting cSA muteins had not been studied enough previously. Furthermore, mutations induced here are different from alanine. These mutations, except for E116N and E116Q, are considered to retain similar electrostatic charges to those of the wild-type (WT) residues and have functional moieties that form similar hydrogen bonds (Table I).[22] Here, we performed thermodynamic analyses to reveal the functions of these cSA muteins and the effects of mutations from a biophysical viewpoint. We evaluated the interaction with biotin by using isothermal titration calorimetry (ITC) and assessed thermodynamic stability by using differential scanning calorimetry (DSC) and sodium dodecyl sulfate–polyacrylamide gel electrophoresis (SDS–PAGE). Our results showed that all of the eight muteins we tested bound biotin in the same manner as does WT cSA, and all muteins maintained the thermodynamic

Table I. *Mutated Residues and the Immunoreactivities of the Resulting Muteins*[a]

Mutein	Mutated residue(s)	Relative immunoreactivity to wild-type cSA (%)
072	Y83S	17
001	R84K	61
083	E116N	126
091	E116Q	113
030	Y83S, R84K, E116N	11
040	Y83S, R84K, E116Q	7
314	Y22S, Y83S, R84K, E101D, R103K, E116N	1
414	Y22S, Y83S, R84K, E101D, R103K, E116Q	1

[a] From Ref. 22.

stabilities of the WT form. The present results suggest that the strategy of mutating surface target sites by preserving electrostatic charge and functional moieties prevents immune recognition while maintaining the structure and function of cSA. This strategy may offer an innovative method for constructing hypoimmunogenic muteins of other proteins for therapeutic applications.

Results

Asymmetric field-flow fractionation–multiangle light scattering analyses of mutant cSAs

Recombinant cSA WT and the muteins listed in Table I were expressed in *Escherichia coli* Rosetta2 (DE3) cells as insoluble forms and were refolded to obtain cSA tetramers by using stepwise dialysis as described previously, with slight modification.[26] Size-exclusion chromatography showed single peaks for all of these proteins except mutein 083, which had a shoulder peak (Supporting Information Fig. S2); this shoulder peak was collected as mutein 083′. Field-flow fractionation–multiangle light scattering (FFF-MALS) analyses to evaluate the molecular sizes and weights of the various cSAs showed that the main peaks identified on size-exclusion chromatography had molecular weights consistent with that of tetrameric cSA WT and that, compared with cSA WT, muteins 314 and 414 might have larger molecular radii in the absence of biotin (Supporting Information Fig. S3).

ITC analyses of cSAs

Because biotin-binding activity is a primary, characteristic property of cSA, we used ITC to measure the thermodynamics of biotin-binding among the hypoimmune muteins [Fig. 2(A)]. The WT form and all of the cSA muteins had very strong binding constants ($K_a > 10^{10}$ M^{-1}) that exceeded the measurement limit of ITC. We note that the values of stoichiometry N were found in the range 1.0–1.2 in all the constructs examined, except that of mutein 083′ (N = 0.8) [Fig. 2(B)]. The binding enthalpies (ΔH_{bind}s) were similar among cSA WT and all muteins (Table II). Therefore, the ITC analyses implied that all muteins other than 083′ had the same biotin-binding characteristics as those of cSA WT.

DSC analyses of cSAs

Thermal stability is an important factor for therapeutic proteins, such as the antibody fragment single-chain Fv.[27] To investigate the thermal stabilities of various cSAs, DSC analyses were carried out. The denaturation temperature (T_M) was estimated as the peak top of heat capacity curves. Accordingly, the T_Ms of cSA WT and the hypoimmunogenic muteins were higher when biotin was bound than in its absence [Fig. 3(A)]. The T_Ms of muteins 314 and 414 were lower than that of WT in both the absence and presence of biotin. In comparison, the T_Ms of muteins 083, 030, and 314, which all contain the mutation E116N, were greatly decreased compared with that of cSA WT, whereas those of muteins 001 and 091 were increased (Table III). Only mutein 083′ yielded multiple peaks on DSC analysis [Fig. 3(B)], indicating that its components contained several tetrameric structures. Although the T_Ms of the hypoimmunogenic muteins were lower than that of cSA WT (Table III), destabilization was negligible, and all muteins demonstrated sufficient thermal stability under the biological condition.

SDS–PAGE analyses of cSAs

To analyze the thermal and chemical stabilities of the hypoimmunogenic muteins in more detail, we performed SDS–PAGE analyses of the various cSAs with stepwise heating from 45 to 95 °C.[28,29] Streptavidin retains its tetrameric structure even during SDS–PAGE after heating of samples at low temperature.[28,29] The tetrameric band in SDS–PAGE dissociates to a monomeric band only after heating samples at high temperatures thus indicating the thermal stability of streptavidin.[28,29]

Stepwise increases in the sample-heating temperature were associated with progressive migration from high- to low-molecular-weight bands (Fig. 4). The temperatures at which this migration began coincided well with the denaturation temperature determined from the DSC data [Fig. 4(A) and Supporting Information Fig. S6]. Unlike cSA WT and all other muteins, mutein 083′ showed multiple bands at low temperatures [Fig. 4(B)], indicating that this sample may contain several different oligomeric assemblies. The ease with which the high-molecular-weight bands and their migration temperatures could be appreciated indicated that the cSA muteins had sufficient thermal and chemical stability for this analysis, thus indicating the considerable stabilities of cSAs. However, all muteins except cSA WT, mutein 001, and mutein 091 yielded faint low-molecular-weight bands at low temperatures [Fig. 4(A) and Supporting Information Fig. S6), suggesting that the induced mutations slightly decreased the muteins' chemical stability to the denaturant SDS.

Discussion

Few previous studies have investigated the biophysical properties of cSA muteins in detail. Here, we assessed the thermodynamic properties of several cSA muteins that have low immunoreactivities.

ITC implied that biotin-binding activity was similar among cSA WT and all of the muteins we evaluated (Table II). The migrations of T_M due to biotin binding were consistent with those of previous reports (Table III).[3,4] SDS–PAGE analysis showed considerable stabilities (Fig. 4). Because cSA

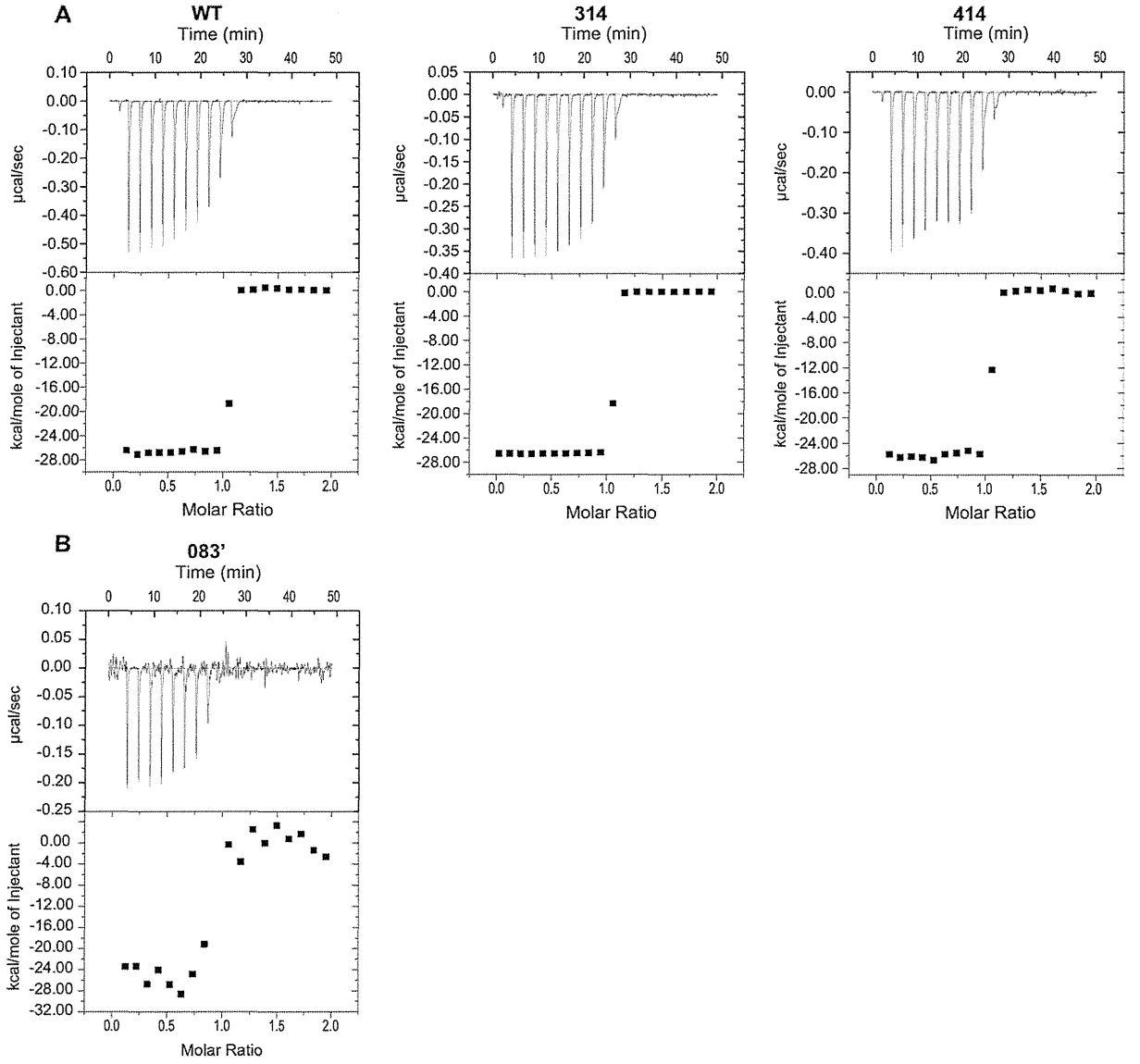

Figure 2. Results of ITC. K_a exceeded the measurement limit of ITC, and ΔS could not be calculated. (A) cSA WT (left); mutein 314 (middle); and mutein 414 (right). (B) 083′.

requires a strict tetrameric structure for high biotin-binding affinity,[19] we concluded that the induced mutations do not disrupt the conformational relationships required for biotin binding. While the R84I mutation has been reported to cause decreased biotin-binding activity compared with that of cSA WT,[18] the R84K variation (mutein 001) did not radically affect K_a or ΔH_{bind} in the current study. This difference may reflect differences in electrostatic charge and functional moieties between isoleucine and lysine. Lysine is similar in electrostatic charge to arginine and likewise carries N—H bonds in its side chain, which enables it to form similar hydrogen bonds. In contrast, isoleucine is apparently unable to form hydrogen bonds because it carries only C—H bonds in its side chain.

The mutation E116N (mutein 083) greatly destabilized the resulting cSA protein in stability analyses (Table III), and mutein 083′ showed depression of binding stoichiometry and tetramerization [Figs. 2(B), 3(B), and 4(B)]. In contrast, the mutation E116Q (mutein 091) stabilized the protein (Table III and Supporting Information Fig. S6). This pronounced difference between mutations at E116 and other mutations also seems to reflect the differences in electrostatic

Table II. *Results of ITC*

Mutein	Stoichiometry (N)	ΔH_{bind} (kcal mol^{-1})
WT	1.0	–26.7
072	1.1	–27.3
001	1.0	–25.3
083	1.1	–25.2
083′	0.8	–25.4
091	1.1	–26.8
030	1.2	–26.2
040	1.1	–27.8
314	1.0	–26.6
414	1.0	–26.0